

Supplementary Information for “Causes of ferroelectricity in HfO₂-based thin films: An *ab initio* perspective”

Mehmet Dogan^{1,2,3,4}, Nanbo Gong^{1,5}, Tso-Ping Ma^{1,5} and Sohrab Ismail-Beigi^{1,2,6,7}

¹Center for Research on Interface Structures and Phenomena, Yale University, New Haven, Connecticut 06520, USA

²Department of Physics, Yale University, New Haven, Connecticut 06520, USA

³Department of Physics, University of California, Berkeley, California 94720, USA

⁴Materials Science Division, Lawrence Berkeley National Laboratory, Berkeley, California 94720, USA

⁵Department of Electrical Engineering, Yale University, New Haven, Connecticut 06520, USA

⁶Department of Applied Physics, Yale University, New Haven, Connecticut 06520, USA

⁷Department of Mechanical Engineering and Materials Science, Yale University, New Haven, Connecticut 06520, USA

Oxygen coordination for dopants in HfO₂

We list the dopant-O distances for the nearest oxygens in the 3.125% doped HfO₂ for C, N, N* (N -1e), Al, Al* (Al +1e), Ti and Ge doping in table [S1](#); and for Sr, Sr* (Sr +2e), Y, Y* (Y +1e), La and La* (La +1e) doping in table [S2](#).

Phase	Nearest O neighbor distances (\AA)								C. N.
mono C	1.28	1.31	1.36	2.67	2.70	2.74	2.85		3
ortho C	1.27	1.35	1.37	2.48	2.57	2.66	2.70		3
tetra C	1.45	1.45	1.45	1.45	2.86	2.86	2.86	2.86	4
mono N	1.26	1.31	1.71	2.62	2.79	2.85	2.96		2
ortho N	1.15	2.08	2.15	2.40	2.56	2.56	2.63		1
tetra N	1.24	1.24	1.95	2.18	2.74	2.74	2.75	2.76	2
mono N*	1.24	1.25	1.30	2.60	3.02	3.08	3.17		3
ortho N*	1.24	1.29	1.30	2.63	2.66	2.72	2.91		3
tetra N*	1.27	1.28	1.28	2.33	2.62	2.84	2.84	2.88	3
mono Al	1.87	1.92	1.95	2.03	2.06	2.16	2.81		5
ortho Al	1.91	1.96	1.97	2.00	2.01	2.09	2.79		5
tetra Al	1.83	1.83	1.83	1.83	2.64	2.64	2.64	2.64	4
mono Al*	1.88	1.94	1.95	2.04	2.06	2.19	2.82		5
ortho Al*	1.94	1.95	1.97	1.99	2.03	2.12	2.87		5
tetra Al*	1.83	1.83	1.83	1.83	2.71	2.71	2.71	2.71	4
mono Ti	1.92	1.96	2.06	2.07	2.10	2.25	2.27		5
ortho Ti	1.88	2.03	2.04	2.07	2.09	2.24	2.30		5
tetra Ti	1.88	1.88	1.88	1.88	2.58	2.58	2.58	2.58	4
mono Ge	1.88	1.88	1.94	1.95	1.99	2.22	2.84		5
ortho Ge	1.87	1.92	1.93	1.93	1.99	2.17	2.90		5
tetra Ge	1.81	1.81	1.81	1.81	2.69	2.69	2.69	2.69	4

Table S1: List of (C, N, N*, Al, Al*, Ti, Ge)-O bond lengths for each of the monoclinic, orthorhombic and tetragonal phases, for the 3.125% doped HfO_2 . The number of oxygen neighbors to the dopant (coordination number) is reported in the rightmost column. It is assumed that if the distance between the two atoms is not much larger than the sum of their atomic radii, the two atoms are coordinated.

Phase	Nearest O neighbor distances (Å)								C. N.
mono Sr	2.31	2.31	2.33	2.43	2.43	2.43	2.46		7
ortho Sr	2.32	2.35	2.40	2.41	2.43	2.45	2.46		7
tetra Sr	2.38	2.38	2.38	2.38	2.50	2.50	2.50	2.50	8
mono Sr*	2.32	2.32	2.38	2.43	2.46	2.47	2.49		7
ortho Sr*	2.32	2.38	2.42	2.42	2.45	2.46	2.52		7
tetra Sr*	2.40	2.40	2.40	2.40	2.55	2.55	2.55	2.55	8
mono Y	2.17	2.19	2.27	2.27	2.29	2.34	2.36		7
ortho Y	2.18	2.24	2.27	2.27	2.29	2.33	2.36		7
tetra Y	2.24	2.24	2.24	2.24	2.42	2.42	2.42	2.42	8
mono Y*	2.17	2.19	2.27	2.28	2.30	2.35	2.37		7
ortho Y*	2.19	2.27	2.28	2.30	2.34	2.38	2.50		7
tetra Y*	2.24	2.24	2.24	2.24	2.44	2.44	2.44	2.44	8
mono La	2.23	2.25	2.34	2.35	2.36	2.40	2.44		7
ortho La	2.25	2.30	2.34	2.36	2.39	2.40	2.42		7
tetra La	2.31	2.31	2.31	2.31	2.47	2.47	2.47	2.47	8
mono La*	2.24	2.25	2.33	2.38	2.39	2.43	2.45		7
ortho La*	2.22	2.31	2.38	2.38	2.39	2.44	2.47		7
tetra La*	2.32	2.32	2.32	2.32	2.49	2.49	2.49	2.49	8

Table S2: List of (Sr, Sr*, Y, Y*, La and La*)-O bond lengths for each of the monoclinic, orthorhombic and tetragonal phases, for the 3.125% doped HfO₂. The number of oxygen neighbors to the dopant (coordination number) is reported in the rightmost column. It is assumed that if the distance between the two atoms is not much larger than the sum of their atomic radii, the two atoms are coordinated.

Energy vs matching area curves for (Al, Ge, Ti, La):HfO₂

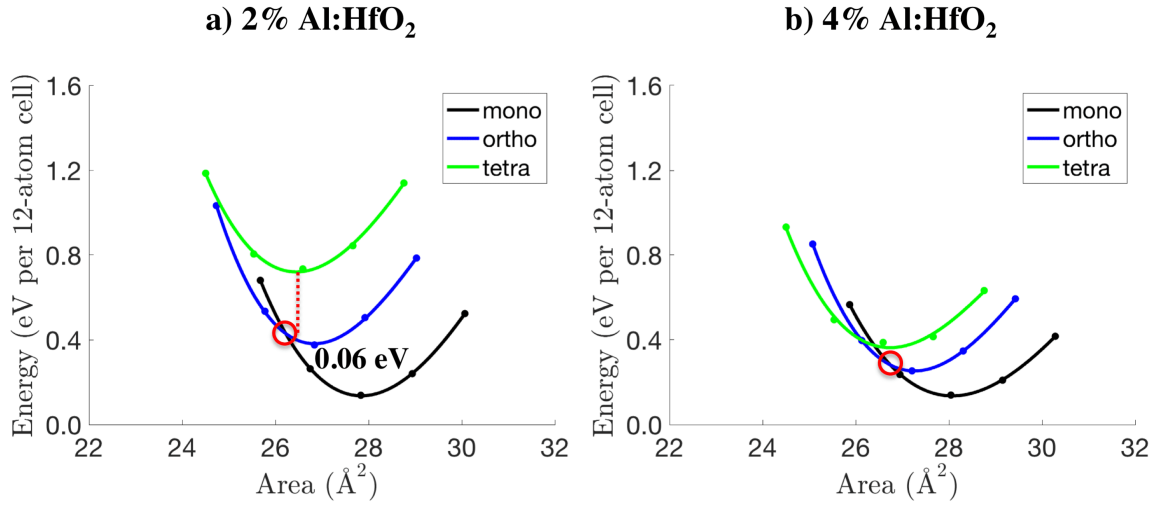


Figure S1: Energies of the monoclinic, orthorhombic and tetragonal phases vs in-plane matching area for epitaxially strained bulk simulations of (a) 2% Al doped and (b) 4% Al doped HfO_2 . For each composition and phase, five data points at -4%, -2%, 0%, 2% and 4% strain are chosen and computed (circular marks). The curves are obtained by fitting cubic polynomials to these five data points. The energy difference between the orthorhombic and the monoclinic phases at the optimized area of the t [100] grain is labelled in the figure in (a), and is equal to zero in (b). The zero of energy is chosen arbitrarily.

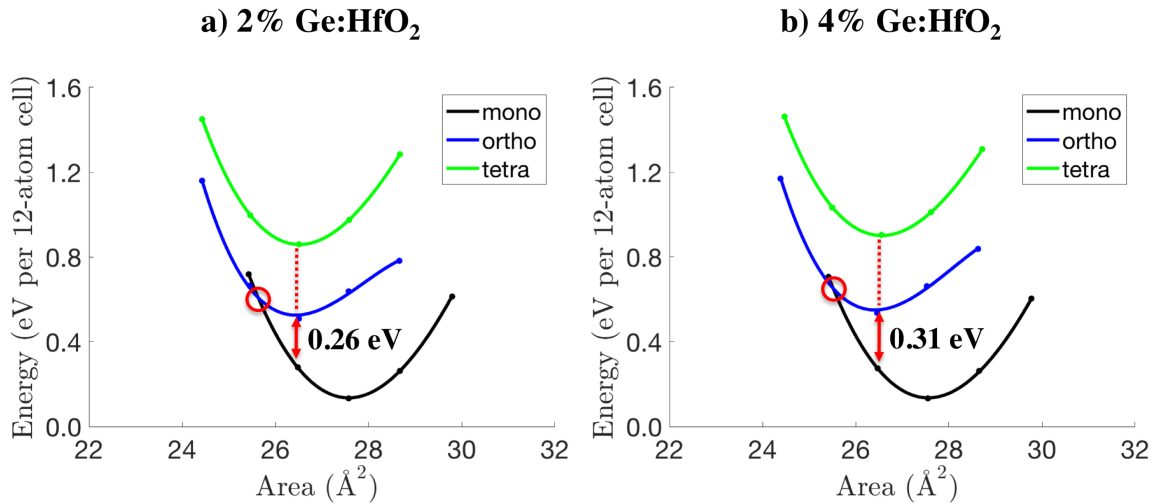


Figure S2: Energies of the monoclinic, orthorhombic and tetragonal phases vs in-plane matching area for epitaxially strained bulk simulations of (a) 2% Ge doped and (b) 4% Ge doped HfO_2 . For each composition and phase, five data points at -4%, -2%, 0%, 2% and 4% strain are chosen and computed (circular marks). The curves are obtained by fitting cubic polynomials to these five data points. The energy difference between the orthorhombic and the monoclinic phases at the optimized area of the t [100] grain is labelled in the figure. The zero of energy is chosen arbitrarily.

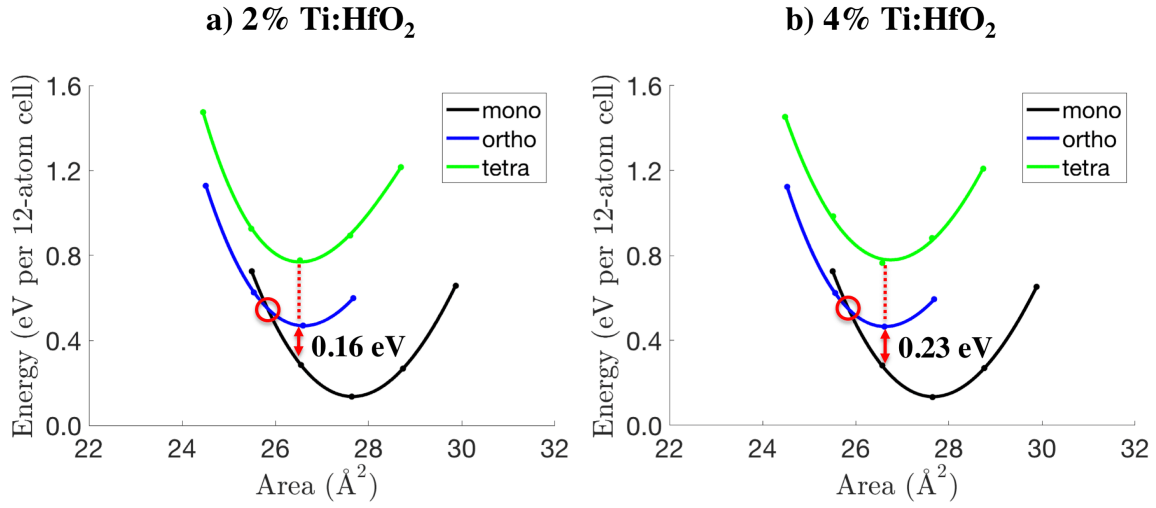


Figure S3: Energies of the monoclinic, orthorhombic and tetragonal phases vs in-plane matching area for epitaxially strained bulk simulations of (a) 2% Ti doped and (b) 4% Ti doped HfO_2 . For each composition and phase, five data points at -4%, -2%, 0%, 2% and 4% strain are chosen and computed (circular marks). The curves are obtained by fitting cubic polynomials to these five data points. The energy difference between the orthorhombic and the monoclinic phases at the optimized area of the t [100] grain is labelled in the figure. The zero of energy is chosen arbitrarily.

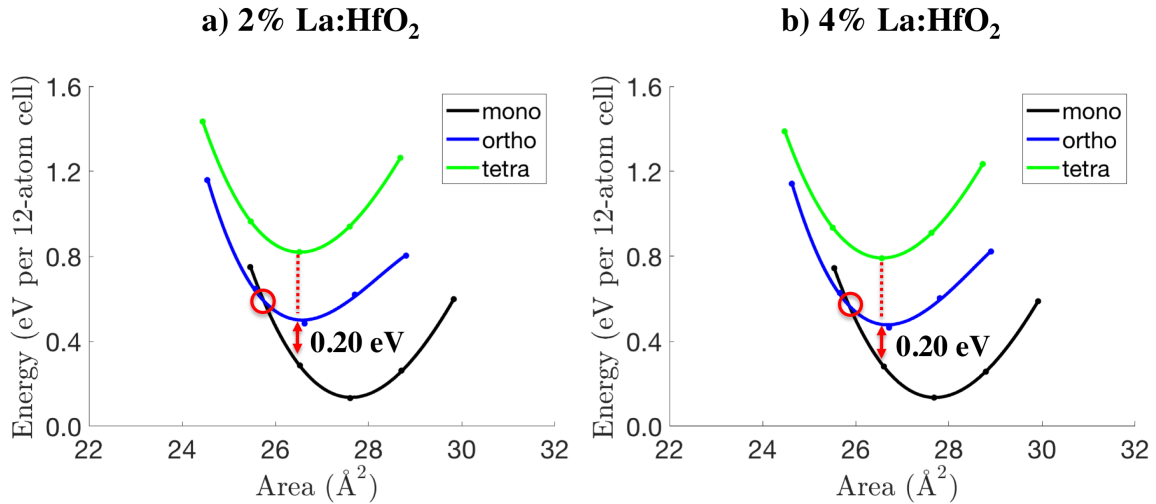


Figure S4: Energies of the monoclinic, orthorhombic and tetragonal phases vs in-plane matching area for epitaxially strained bulk simulations of (a) 2% La doped and (b) 4% La doped HfO_2 . For each composition and phase, five data points at -4%, -2%, 0%, 2% and 4% strain are chosen and computed (circular marks). The curves are obtained by fitting cubic polynomials to these five data points. The energy difference between the orthorhombic and the monoclinic phases at the optimized area of the t [100] grain is labelled in the figure. The zero of energy is chosen arbitrarily.